Author's Accepted Manuscript

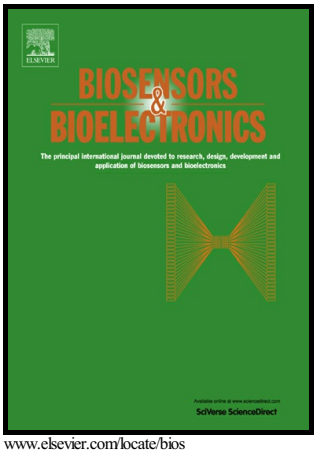

www.elsevier.com/locate/bios

Fabrication of Sensitive Bioelectrode Based on Atomically Thin CVD Grown Graphene for Cancer Biomarker Detection

Vijay K. Singh, Saurabh Kumar, Sumit Kumar Pandey, Saurabh Srivastava, Monu Mishra, Govind Gupta, B.D. Malhotra, R.S. Tiwari, Anchal Srivastava

PII: S0956-5663(18)30018-6
DOI: https://doi.org/10.1016/j.bios.2018.01.014
Reference: BIOS10207

To appear in: *Biosensors and Bioelectronic*

Received date: 25 October 2017
Revised date: 5 January 2018
Accepted date: 8 January 2018

Cite this article as: Vijay K. Singh, Saurabh Kumar, Sumit Kumar Pandey, Saurabh Srivastava, Monu Mishra, Govind Gupta, B.D. Malhotra, R.S. Tiwari and Anchal Srivastava, Fabrication of Sensitive Bioelectrode Based on Atomically Thin CVD Grown Graphene for Cancer Biomarker Detection, *Biosensors and Bioelectronic,* https://doi.org/10.1016/j.bios.2018.01.014

This is a PDF file of an unedited manuscript that has been accepted for publication. As a service to our customers we are providing this early version of the manuscript. The manuscript will undergo copyediting, typesetting, and review of the resulting galley proof before it is published in its final citable form. Please note that during the production process errors may be discovered which could affect the content, and all legal disclaimers that apply to the journal pertain.

ACCEPTED MANUSCRIPT

Fabrication of Sensitive Bioelectrode Based on Atomically Thin CVD Grown Graphene for Cancer Biomarker Detection

Vijay K. Singh[a], Saurabh Kumar[b], Sumit Kumar Pandey[a], Saurabh Srivastava[b], Monu Mishra[c], Govind Gupta[c], B.D. Malhotra[b], R.S.Tiwari[a*], Anchal Srivastava[a*]

[a]Department of Physics, Institute of Science, Banaras Hindu University, Varanasi– 221005,India

[b]Nanobioelectronics Laboratory, Department of Biotechnology, Delhi Technological University, Shahbad Daulatpur, Delhi - 110042, India

[c]Advanced Materials and Devices Division, CSIR-National Physical Laboratory, Dr. K. S. Krishnan Marg, New Delhi – 110012, India.

Abstract:

Motivation behind the present work is to fabricate a cost effective and scalable biosensing platform for an easy and reliable detection of cancer biomarker Carcinoembryonic antigen (CEA). Here, we report the sensitive and selective detection of CEA using graphene based bio-sensing platform. Large sized (~2.5 x 1.0 cm^2), uniform, continuous, single and few layers graphene films have been grown on copper (Cu) substrate employing chemical vapor deposition (CVD) technique using hexane as a liquid precursor. Functional group has been created over Graphene/Cu substrate through π-π stacking of 1- pyrenebutanoic acid succinimidyl ester (PBSE). Further, to make the sensor specific to CEA, antibody of CEA (anti-CEA) has been covalently immobilized onto PBSE/Graphene/Cu electrode. Selective and sensitive detection of CEA is achieved by anti-CEA/PBSE/Graphene/Cu electrode through electrochemical impedance spectroscopy (EIS) measurements. Under optimal condition, the fabricated sensor shows linear response in the physiological range 1.0 - 25.0 ng mL^{-1} (normal value ~5.0 ng mL^{-1}), revealing sensitivity 563.4 Ω ng^{-1} mL cm^{-2} with a correlation coefficient of 0.996 and limit of detection (LOD) 0.23 ng mL^{-1}. In this way, one step electrode fabrication with high specific surface area provides a light weight, low cost, reliable and scalable novel

Accepted manuscript

ACCEPTED MANUSCRIPT

biosensing platform for sensitive and selective detection of CEA. We believe that this bioelectrode equipped with specific recognition elements could be utilized for detection of other biomolecules too.

Keywords: Graphene, CEA, EIS, Label-free detection, Biosensor.

*Corresponding authors:

E-Mail ID: rstiwariphy@yahoo.com (Prof. R.S. Tiwari), anchalbhu@gmail.com (Prof. Anchal Srivastava) Phone No.: +91-9415991746, +91-9453203122,

1. Introduction:

Cancer disease, characterized by the uncontrolled growth and spread of abnormal cells, is one of the major threats to the human life worldwide. The early and accurate detection of cancer is extremely important for clinical diagnosis, effective toxicity monitoring, and ultimately for the successful treatment of cancer. CEA is one of the cancer biomarkers, which has been extensively used for diagnostic purposes in gastrointestinal, breast and lung cancer (Aquino et al. 2004; Duffy 2001). In an adult nonsmoker human serum, the normal level of CEA is less than 2.5 ng mL^{-1} and for a smoker it is less than 5.0 ng mL^{-1} (Loewenstein and Zamcheck 1978; Su et al. 2008). The accurate and sensitive detection of CEA level can lead to the diagnosis of cancer in its early stage. In recent years, immense efforts have been made for the development of CEA sensing methods with high sensitivity and specificity (Liu et al. 2012; Zhang and Cui 2011; Zheng et al. 2005). In comparison to the presently used methods specifically, the polymerase chain reaction method, culturing and colony counting method, and the enzyme-linked immunosorbent assay (ELISAs) which are tiresome and need more time (typically hours to days), on the other hand the bioelectrode based biosensing approach offers rapid and sensitive measurements. Several nanoelectronic biosensors have been developed based on various

Accepted manuscript

ACCEPTED MANUSCRIPT

nanostructured materials such as nanowires (Wanekaya et al. 2006; Zhang et al. 2011; Zhang et al. 2010a; Zhang et al. 2010b; Zheng and Lieber 2011), nanotubes (Allen et al. 2007; Singh et al. 2013), quantum dots (Hansen et al. 2006; Yang et al. 2012), graphene oxide (GO) (Feng et al. 2011; Jung et al. 2010), reduced graphene oxide (RGO) (Kumar et al. 2015; Zhou et al. 2009) etc. However, bioelectrodes based on these nanomaterials suffer several drawbacks such as, bioelectrode fabrication of these materials requires some supporting substrate such as indium tin oxide (ITO), glassy carbon electrode (GCE), and gold electrodes etc., which are costly and also requires costly binders (nafion) as an adhesive materials.

The discovery of graphene by Geim et al. (Geim 2009), which is a flat atomically thin sheet of carbon atoms arranged in two-dimensional (2D) honeycomb lattice, has stimulated a huge amount of research in biosensing due to its extraordinary structural, electrical, physical, optical and biocompatible properties (Huang et al. 2011; Lee et al. 2008; Neto et al. 2009a; Neto et al. 2009b). Graphene has also added a new dimension to the field of electrochemical sensing because of its perfect 2D structure, which provides large detection area and enables facile and homogeneous functionalization of a variety of aromatic biomolecules through $\pi - \pi$ interaction (Van der Waals force) (Ajayan and Tour 2007). Graphene based devices have potential of portability, rapid diagnostic point-of-care sensing compared to the presently used ELISAs which are time consuming and labor intensive.

For realizing any potential applications of graphene, an easy and less toxic synthesis method is required. Till date, several synthesis methods for producing graphene have been reported such as; mechanical exfoliation (Novoselov et al. 2004), chemical exfoliation (Schniepp et al. 2006), chemical vapor deposition (CVD) (Srivastava et al. 2010) etc. Among these, CVD is one of the novel synthesis routes for producing good quality, large area, mono and few layers

Accepted manuscript

ACCEPTED MANUSCRIPT

graphene. The advantage of CVD grown graphene over other chemically derived graphene such as RGO, GO etc. is that it gives one atom thick, monolithic and continuous membrane without any discontinuity. This also facilitates reproducibility while scaling it from laboratory to industry which is a major challenge for the synthesis of most of the nanomaterials.

Keeping the above points in view, in this work, good quality large area mono and few layers graphene films have been synthesized on Cu substrate adopting liquid precursor CVD route (Srivastava et al. 2010). To the best of our knowledge, there is no report of using graphene directly on metallic substrate as biosensing platform. In the present method, as synthesized graphene films on Cu substrate have been used as an electrode material, which does not require any further tedious processing such as transferring of graphene onto an insulating substrate SiO_2/Si etc. However, there are several techniques for electrode fabrication from precursor material such as spin coating, electrophoretic deposition, screen printing, inkjet printing etc.(Ge et al. 2012; Kumar et al. 2013; Setti et al. 2005; Zhang et al. 2000), but these techniques are costly, require sophisticated instrumentations and not scalable too. Few reports are also available on graphene based FET devices (Feng et al. 2013; Sui and Appenzeller 2009; Yang et al. 2010; Yeh et al. 2016), but such devices require transferring of graphene from metallic to SiO_2/Si substrate. This process creates many wrinkles and defects in graphene film, which greatly reduces the electrical conductivity and hence potential performance of graphene. Such device fabrication is also very tedious and not cost effective. Therefore, one step electrode fabrication employed in the present work is an added advantage over other known methods of electrode fabrication. The bioelectrode fabricated on metal substrate in present study is also environment friendly and there is no issue of disposability. Further, this CVD synthesized graphene on Cu substrate has been applied to demonstrate as an efficient, easy and reliable label free biosensing

Accepted manuscript

ACCEPTED MANUSCRIPT

platform for detection of CEA with high sensitivity and specificity having the potential of scalability (Table-1).

2. Materials and methods

2.1.Synthesis of graphene

Large-sized graphene films were grown on Cu foils by CVD technique using hexane as a liquid precursor for carbon (Srivastava et al. 2010). Cu foils were loaded into a quartz tube furnace and initially quartz tube was purged with hydrogen (H_2) gas at a constant flow of 100 sccm. Furnace temperature was raised up to 980 ºC under a constant heating rate of 20 ºC/min. Temperature of the furnace was stabilized at 980 ºC for 30 minutes to anneal the Cu foil. Further, CVD growth of graphene was started by directing hexane vapor for 5 min into the furnace, followed by cooling the furnace to the room temperature under the H_2 atmosphere.

2.2.Fabrication of Immunosensor (anti-CEA/PBSE/Graphene/Cu)

Graphene/Cu electrode was dipped into the PBSE solution (2 mg mL^{-1}) for 2 h. The PBSE was used as the noncovalent functionalization reagent, which adsorbed onto the graphene sheets through π-π stacking resulting in a stable PBSE-graphene composite. The functional groups of PBSE were used to conjugate antibodies of CEA to form anti-CEA/PBSE/Graphene/Cu electrode (Chen et al. 2001; Yang et al. 2008; Yang and Gong 2010). The anti-CEA antibodies (30 µL, 100 µg mL^{-1} in phosphate buffer; 50 mM, pH 7.2, 0.9% NaCl) were covalently immobilized onto PBSE/Graphene/Cu electrode as shown in Fig.1. The anti-CEA/PBSE/Graphene/Cu was then rinsed with phosphate buffer (PBS, 50 mM, pH 7.2, 0.9% NaCl) to remove the unbounded antibodies, and 1% of bovine serum albumin (BSA) in PBS was added to the antibody-modified electrode to block unspecific sites. After rinsing again with PBS, electrodes were stored at 4 °C.

Accepted manuscript

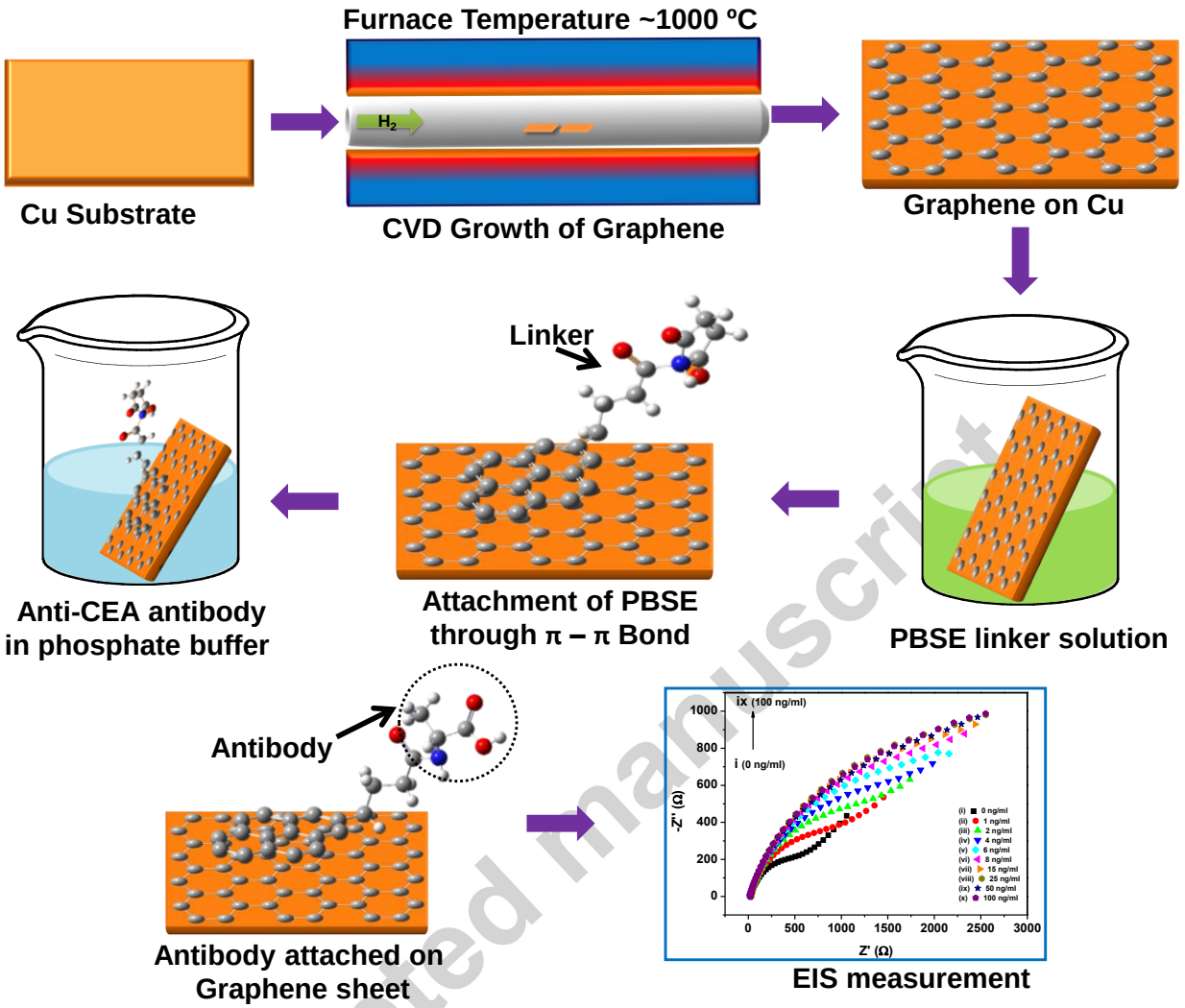

Fig.1. Schematic of biosensor fabrication and EIS measurements.

2.3.Characterization

The surface morphology of graphene was observed using Optical microscope (Dewinter, Italy), Scanning electron microscope (SEM) (ZEISS, Germany), Transmission electron microscope (TEM) (FEI, USA) and Atomic force microscope (AFM) (NT-MDT, Russia). Spectroscopic characterization of the as grown graphene films were carried out using Raman spectroscope (RenishawinVia, Germany). Presence of functional groups on fabricated bioelectrodes were analyzed using Fourier-transform infrared (FTIR) spectrometer (Frontier,

ACCEPTED MANUSCRIPT

Perkin Elmer, USA) in Attenuated total reflectance (ATR) mode. The X-Ray photoelectron spectroscopic (XPS) measurements were performed in Multiprobe Surface Analysis System (Scienta Omicron, Germany) operated at a base pressure of 5 x 10^{-11} Torr. High resolution XPS spectra were recorded using monochromatic AlKα (1486.7 eV) radiation source. The pass energy of the scans were kept at 20 eV with an ultimate spectral resolution of ~0.3 eV. The calibration of spectrometer was performed via standard gold sample as described earlier (Mishra et al. 2017).

The electrochemical behavior of the fabricated biosensors were investigated employing an Autolab Potentiostat/Galvanostat (Metrohm, Netherlands) using a conventional three-electrode cell with the BSA/anti-CEA/PBSE/Graphene/Cu as working electrode, platinum as auxiliary electrode and Ag/AgCl as the reference electrode in phosphate buffer saline (PBS, 50 mM, pH 7.4) containing 5 mM $[Fe(CN)_6]^{3-/4-}$.

3. Results and discussion

3.1. Optical and Electron microscopy

The optical, SEM, TEM and HR-TEM images obtained for the graphene film have been shown in Fig.2. Optical image Fig.2(a) shows that graphene film is homogeneous in large area with wrinkles on its surface. The SEM image Fig. 2(b) shows the presence of few multilayer (ML) islands (darker regions) over the uniform single layer (SL) graphene film. Further, for the TEM investigation, graphene film was transferred from Cu foil to lacey carbon coated TEM grid. TEM analysis reveals that graphene film is uniform with folded layers in few regions Fig.2(c). HR-TEM image shown in Fig.2(d) confirms the presence of 2-3 layers in graphene film, which is consistent with Raman and AFM results.

Accepted manuscript

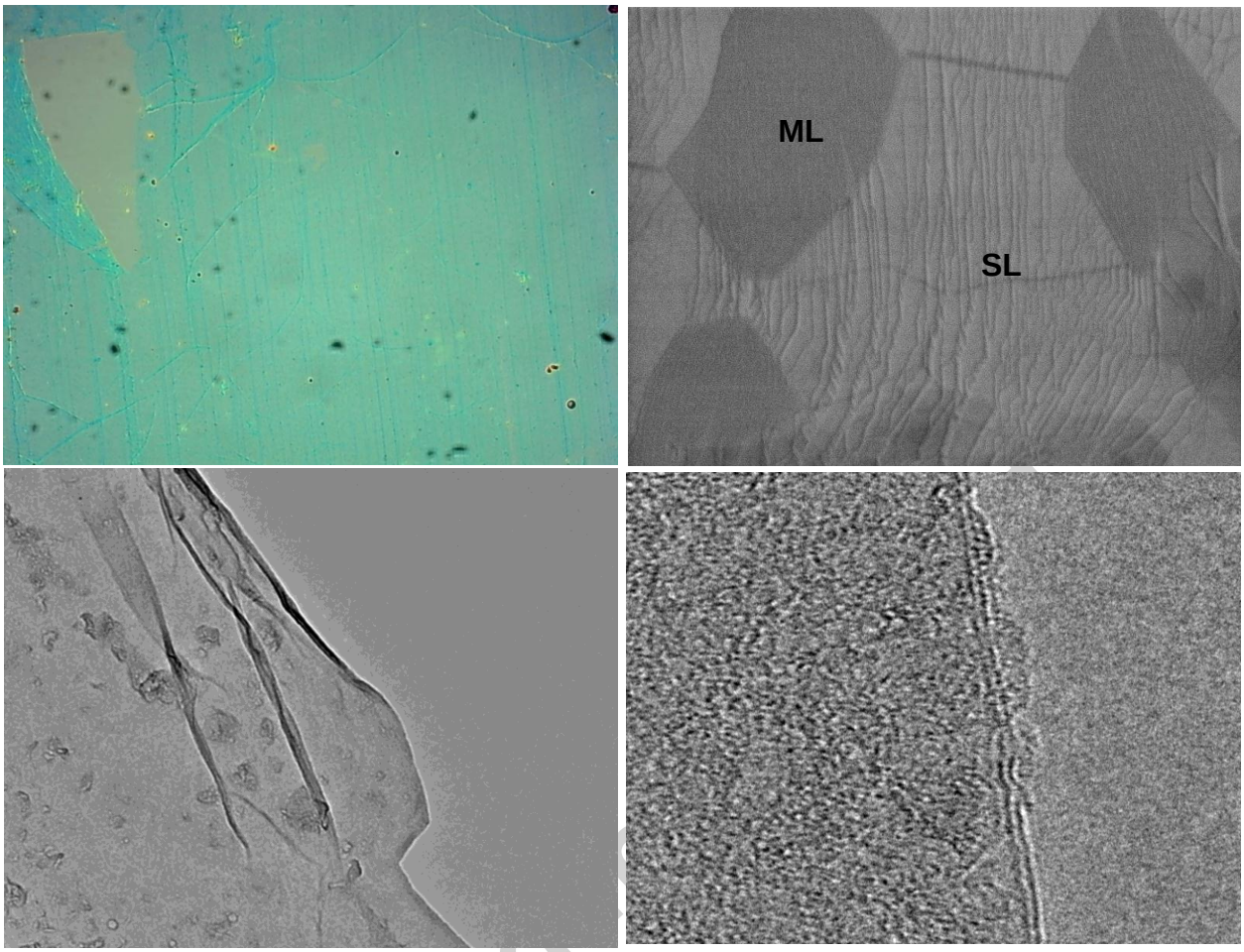

Fig.2. (a) Optical image of graphene film transferred on SiO_2/Si substrate, (b) SEM image showing uniform film of graphene (c) TEM image of graphene film transferred on lacey carbon coated TEM grid where darker region showing folded graphene layer and lighter region indicating the uniform monolayer graphene, (d) HR-TEM image showing bilayer and trilayer graphene films.

Accepted

3.2. AFM analysis

AFM micrograph of graphene (transferred from Cu foil to SiO_2/Si wafer) has been shown in Fig.3(b). In the AFM image, number of wrinkles are visible that may have been emerged during the synthesis due to the wide difference in thermal expansion coefficient of Cu and graphene (Chae et al. 2009). Wrinkles in graphene film may also occur during the transferring

ACCEPTED MANUSCRIPT

process. The thickness profile measurement shown in Fig.3(c) indicates that graphene is 3 layers thick (~1.6 nm) (Novoselov et al. 2004).

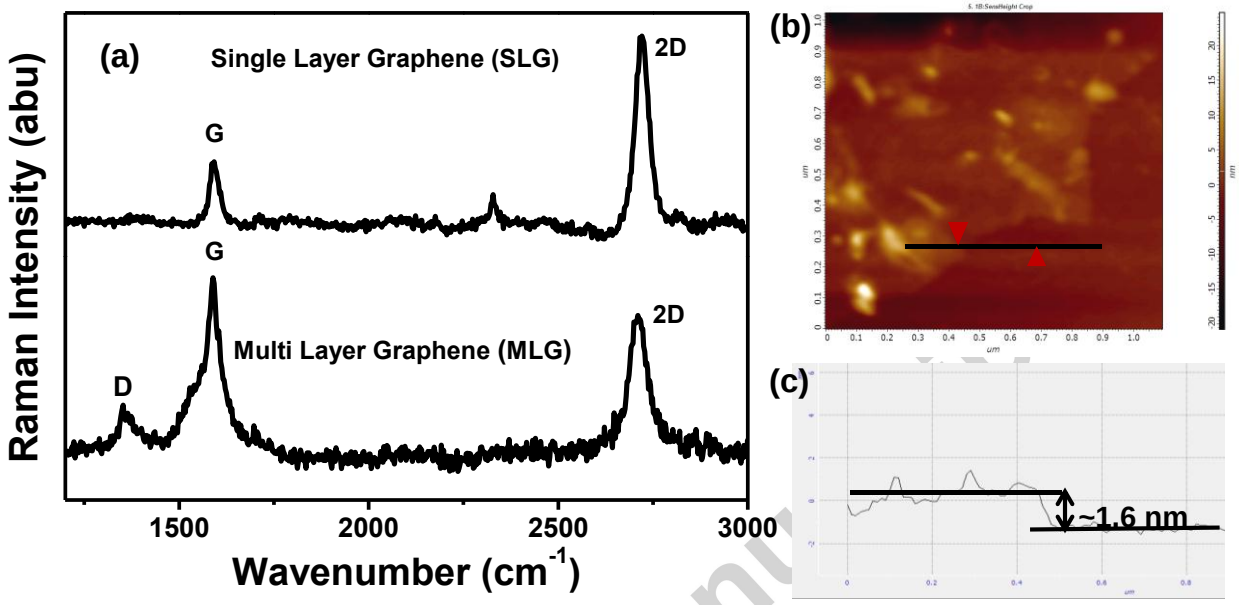

Fig.3. (a) Raman spectra of single and multi-layer graphene, (b) AFM image of graphene, (c) Thickness profile of graphene layer.

3.3. Raman Spectroscopic Analysis

Raman spectroscopy of the as-grown graphene on Cu foil was performed using 514 nm laser excitation to observe the quality and thickness of graphene film and results have been shown in Fig.3(a). The two most prominent peaks observed at ~1590 cm^{-1} and ~2700 cm^{-1} correspond to the G and 2D bands of graphene, respectively. The peak seen at ~1350 cm^{-1} appears due to the defect in graphene film, and known as D band. In our sample, for single layer D band is nearly absent, which indicates that graphene layer is quite homogenous. In the case of multilayer graphene, appearance of D band suggests the presence of few defects in graphene film. Moreover, information regarding the number of layers in graphene film can be extracted from the width and line-shape of 2D band.

ACCEPTED MANUSCRIPT

In the case of single layer graphene, 2D band has Lorentzian shape with FWHM ~42±2 cm^{-1}. Also the intensity ratio of 2D and G band is found to be greater than 2 (i.e. $I_{2D}/I_G>2$), which confirms the presence of single layer graphene (Ferrari et al. 2006; Malard et al. 2009). In multilayer graphene 2D band has FWHM ~ 56±2 cm^{-1} and the intensity ratio of 2D and G band is less than 1 (i.e. $I_{2D}/I_G<1$), which confirms the presence of multilayer islands (darker regions of SEM image) over the single layer graphene on Cu foil.

3.4. FT-IR Analysis

FT-IR spectra of bare Cu, Graphene/Cu, PBSE/Graphene/Cu and anti-CEA/PBSE/Graphene/Cu films have been shown in Fig.4. There are no functional groups present on Cu and Graphene/Cu films. However, in the case of PBSE functionalized Graphene/Cu film (PBSE/Graphene/Cu), peaks at 1154 cm^{-1}, 1268 cm^{-1} correspond to C-O stretching. Peaks at 1407 cm^{-1}, 1335 cm^{-1} and 1514 cm^{-1} are due to O-H bend, symmetric and asymmetric stretching of N-O group of PBSE, respectively. The peak at 2928 cm^{-1} has been assigned to the C-H stretching. After immobilization of anti-CEA on PBSE/Graphene/Cu film characteristic peaks of amide-I and amide-II have been found at 1568 cm^{-1} and 3240 cm^{-1}, respectively (Singh et al. 2013). These amide peaks confirm the functionalization of anti-CEA on PBSE/Graphene/Cu electrode.

Accepted manuscript

ACCEPTED MANUSCRIPT

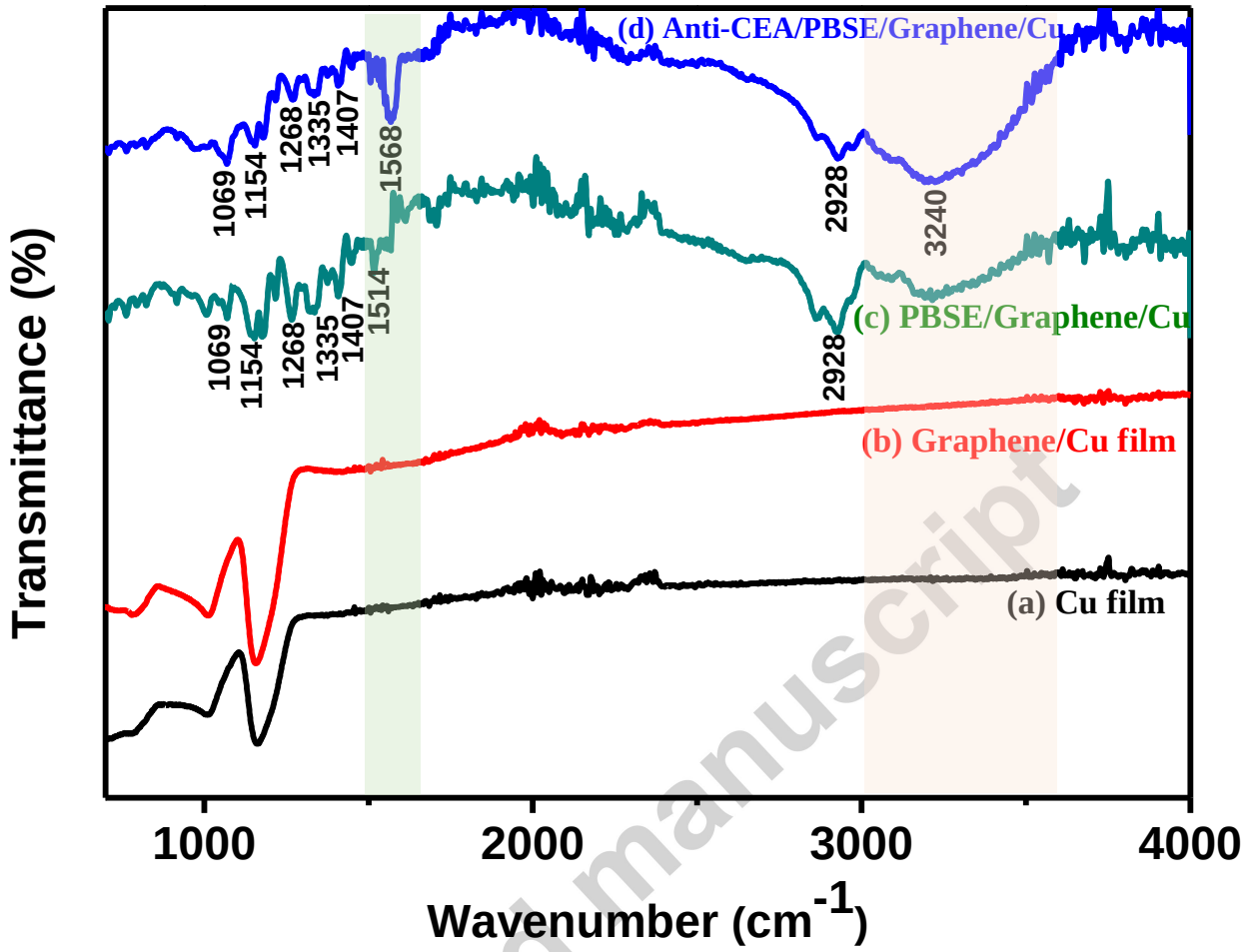

Fig.4. FT-IR spectra of (a) bare Cu film, (b) Graphene/Cu film, (c) PBSE/Graphene/Cu film (d) anti-CEA/PBSE/Graphene/Cu film.

3.5. XPS Studies

An XPS characterization was carried out to study the interaction of PBSE and antibody through graphene layer. The presence of PBSE is confirmed by the characteristic N1s peak at around 400 eV (Fig. 5a) (Liu et al. 2014). The C1s regions of both the electrodes (PBSE/Graphene/Cu and anti-CEA/PBSE/Graphene/Cu electrodes) were deconvoluted into characteristic peaks which have been discussed below.

In the case of PBSE/Graphene/Cu electrode, peaks observed at 284.7 eV, 285.7 eV, 288.8 eV shown in Fig 5(b) correspond to the in-plane sp^2 C=C, C=O and O=C-O bonds, respectively

Accepted manuscript

ACCEPTED MANUSCRIPT

and a weak peak at 286.8 eV is due to the C-N bond present in PBSE. In the anti-CEA/PBSE/Graphene/Cu electrode (Fig. 5c), the binding energy peaks were almost similar to the spectra of the PBSE/Graphene/Cu electrode. Moreover, an additional dominant wide peak seen at 287.9 eV is attributed to the amide bond formation between PBSE terminated graphene sheet and the NH_2 terminated Fab (fragment, antigen-binding) region of anti-CEA (Fig.1) (Singh et al. 2017). The fitting of the XPS spectra of C1s peaks binding energies (eV) and relative atomic percentages (%) of various functional groups present in PBSE/Graphene/Cu and anti-CEA/PBSE/Graphene/Cu films have been summarized in Table S1 in supplementary part. The relative atomic percentage of the C=O group present in the PBSE terminated graphene sample reduces from ~18.5% to ~12.3 % in the anti-CEA/PBSE/Graphene/Cu sample, indicating the removal of succinimide ester (see the supplementary information Fig S2) during covalent bonding with NH_2 terminated Fab region of anti-CEA. Further, the relative atomic percentage of the C-N bond present in PBSE/Graphene/Cu sample increased from ~2.4% to ~19.8 % in anti-CEA/PBSE/Graphene/Cu sample. This may be attributed to the presence of amide bond in the polypeptide chain of antibody (anti-CEA) and amide bond formation between aminated antibody and PBSE terminated graphene.

Accepted manuscript

ACCEPTED MANUSCRIPT

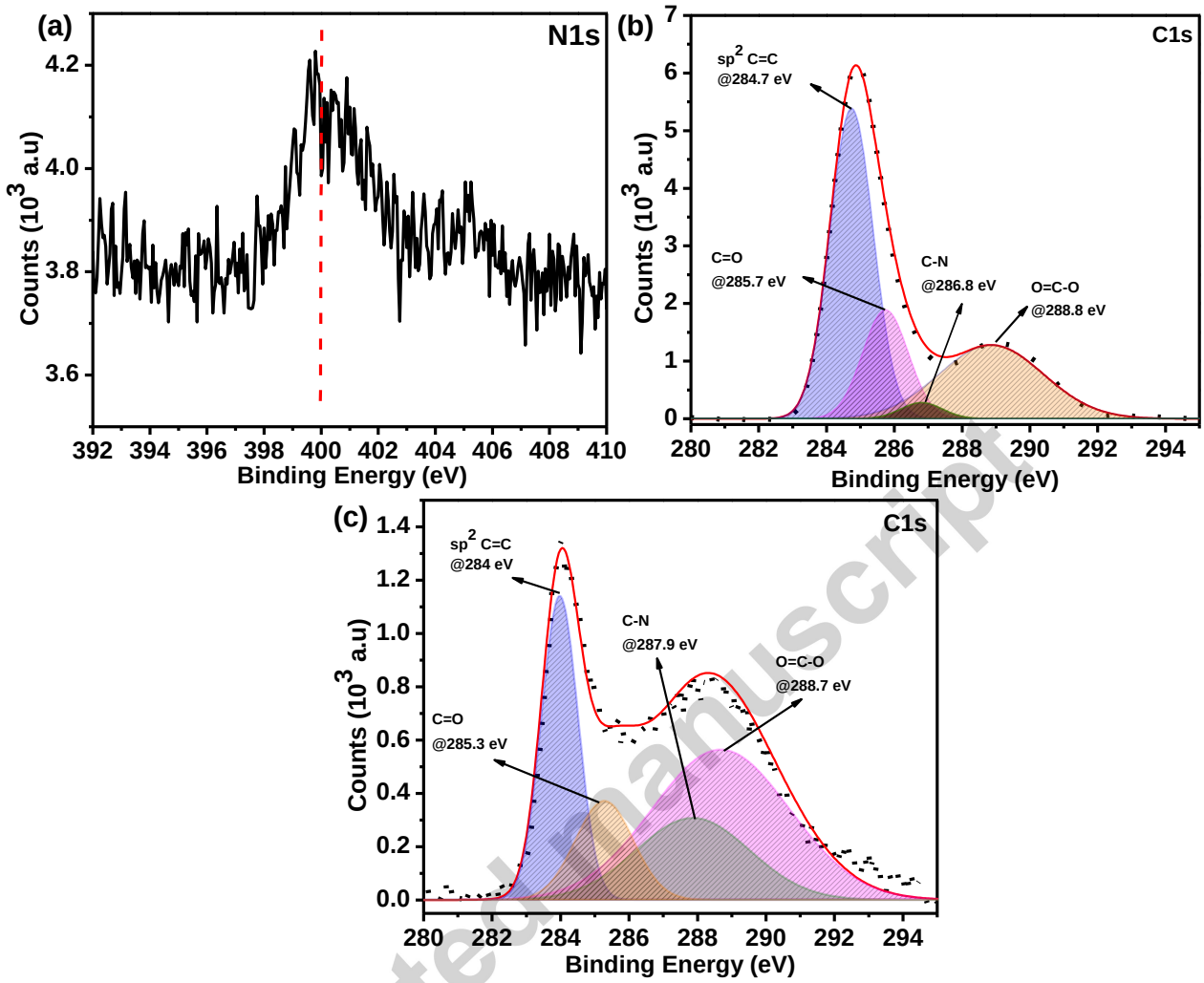

Fig.5. (a) N1s spectrum of PBSE modified graphene and C1s XPS spectrum of (b) PBSE/Graphene/Cu (c) anti-CEA/PBSE/Graphene/Cu.

3.5. Electrochemical Studies

To investigate the charge transfer phenomena at the modified surface/solution interface electrochemical impedance spectroscopy (EIS) were conducted in the frequency range, $1x10^5$-0.1 Hz with amplitude of 0.01. The Randles circuit is mainly used as a fitting model in EIS measurement for the interpretation of the Nyquist plot. It is an equivalent electrical circuit comprising of an active electrolyte resistance (R_S) in series with the parallel combinations of

ACCEPTED MANUSCRIPT

double layer capacitance (C_{dl}) or also replaced with constant phase element (CPE) of a Faradic reaction and charge transfer resistance (R_{CT}) (Randles 1947). The plot obtained between real and imaginary values of impedance is called Nyquist plot and the diameter of semicircle in the Nyquist plot gives the magnitude of charge transfer resistance (R_{CT}) (Moisel et al. 2008). Fig.6(a) shows the Nyquist plot of Cu, Graphene/Cu, PBSE/Graphene/Cu and anti-CEA/PBSE/Graphene/Cu electrodes. The value of R_{CT} for Graphene/Cu is found to be 1.1 KΩ which is lower than that of the Cu electrode (5.6 KΩ). This result indicates that deposition of graphene over Cu electrode enhances the charge transfer from solution to the electrode due to high conductivity and electrochemical behavior of graphene, which increases the permeability of $[Fe(CN)_6]^{3-/4-}$ to the surface of Graphene/Cu electrode. Thus, the modified surface can be correlated with the charge transfer resistance confirming the deposition of graphene over Cu electrode. It can be seen that R_{CT} value for PBSE/Graphene/Cu electrode (2.1 KΩ, curve c) is larger than Graphene/Cu (1.1 KΩ, curve b) electrode. This increase in the R_{CT} value is attributed to the hindrance in charge transfer after PBSE binding. Further, the value of R_{CT} (733.5 Ω, curve d) of the anti-CEA/PBSE/Graphene/Cu immunoelectrode is lower than the PBSE/Graphene/Cu electrode (2.1 KΩ, curve d). The decrease in the value of R_{CT} may be attributed to the spatial orientation of the antibody molecules that perhaps stimulates charge transfer rate to the antibody immobilized surface.

Accepted manuscript

3.6. Electrochemical impedimetric response of the BSA/anti-CEA/PBSE/Graphene/Cu immunoelectrode:

The electrochemical response studies (Fig.6(b)) were conducted on BSA/anti-CEA/ PBSE/Graphene/Cu immunoelectrode as a function of carcinoembryonic antigen (CEA) concentrations (1-100 ng mL^{-1}) in phosphate buffer saline (PBS, 50 mM, pH 7.4, 0.9% NaCl) using EIS. The magnitude of R_{CT} was found to be increased after addition of CEA which may be

attributed to the formation of electrically insulating immunocomplex, produced from the specific antigen-antibody interaction (CEA - anti-CEA immunocomplex) blocking electron transfer. Fig.6(c),(d) show the calibration curves obtained between R_{CT} and CEA concentrations, revealing linearity from 1-25 ng mL^{-1} having sensitivity of 563.4 Ω ng^{-1} mL cm^{-2} with a correlation coefficient of 0.996. Detection limit of the biosensor has been calculated using equation (S1) and LOD is found to be 0.23 ng mL^{-1}.

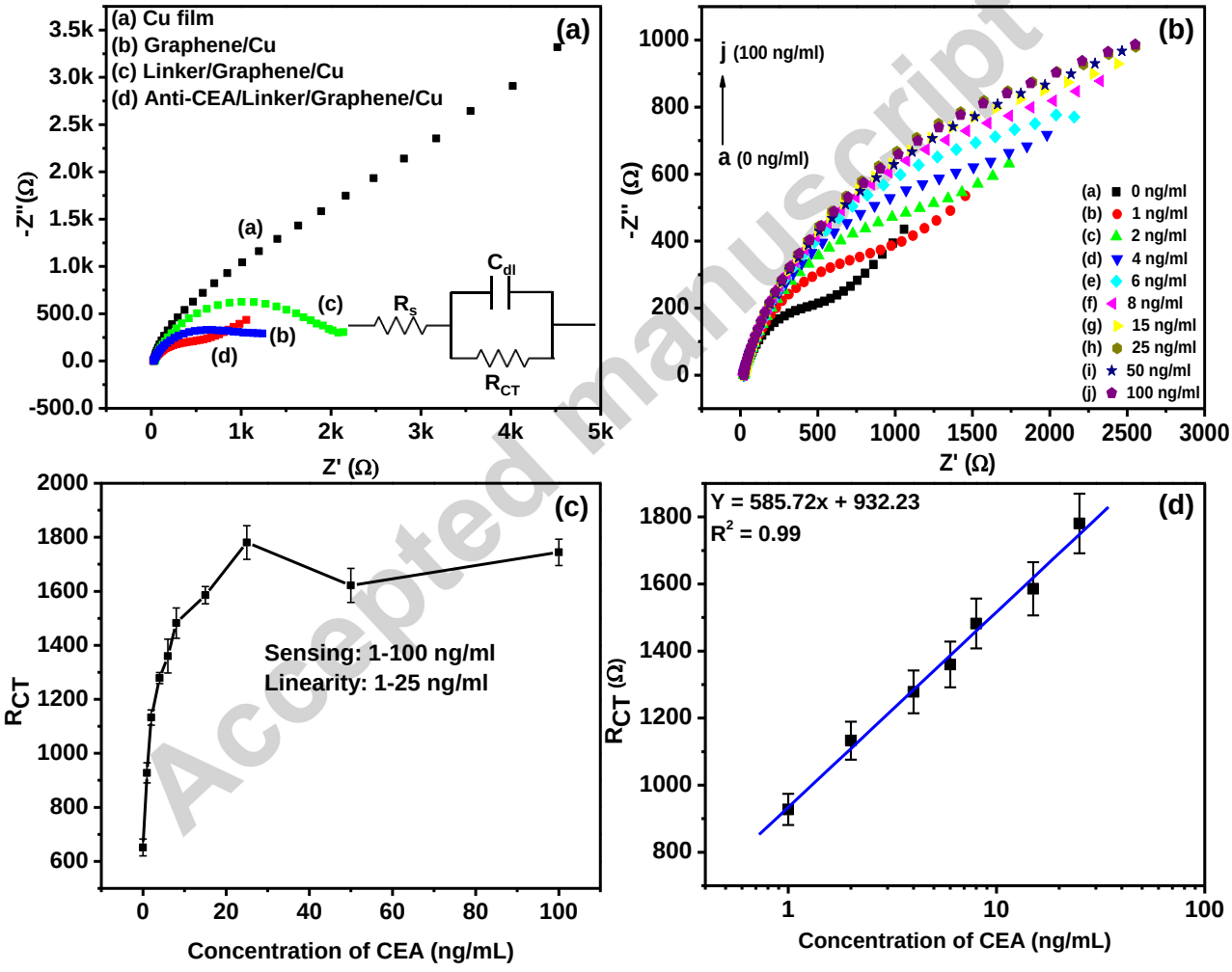

Fig.6. (a) Electrochemical impedance spectra of Cu, Graphene/Cu, PBSE/Graphene/Cu, anti-CEA/ PBSE/Graphene/Cu. (b) Electrochemical response studies of BSA/anti-CEA/PBSE/Graphene/Cu bioelectrode obtained as a function of CEA concentrations (1-100 ng mL^{-1}) and (c) R_{CT} with

ACCEPTED MANUSCRIPT

respect to CEA concentrations (d) calibration plot between R_{CT} recorded at various CEA concentrations.

3.7. Reproducibility, selectivity and stability studies:

The reproducibility of the BSA/anti-CEA/PBSE/Graphene/Cu immunoelectrode was investigated by measuring the EIS response in the presence of CEA (25 ng mL^{-1}) on four independently fabricated immunoelectrodes under identical conditions (Fig. 7(a)). The reproducibility is evaluated in terms of relative standard deviation (RSD). An average R_{CT} of 1850.1 Ω with a RSD of 3.20 % has been found (Fig. 6(b)), which is within the acceptable error range under the tested conditions, suggesting a good reproducible assay.

The selectivity of the fabricated sensor has been examined by monitoring the R_{CT} responses of immunoelectrodes in presence of different interferents present in blood serum such as KCl (8.38 mM), CYFRA-21-1 (2.0 ng mL^{-1}) and CTnI (10.0 ng mL^{-1}) as shown in Fig 7(c). Upon addition of 1.0 ng mL^{-1} CEA, the significant change in the R_{CT} value of immunoelectrode was found. However, upon successive addition of the KCl, CYFRA-21-1 and CTnI interferents, no prominent changes in R_{CT} values have been observed. This indicates that the BSA/anti-CEA/PBSE/Graphene/Cu immunoelectrode specifically interacts with CEA and the response is not affected due to the presence of other potential interferents.

Accepted manuscript

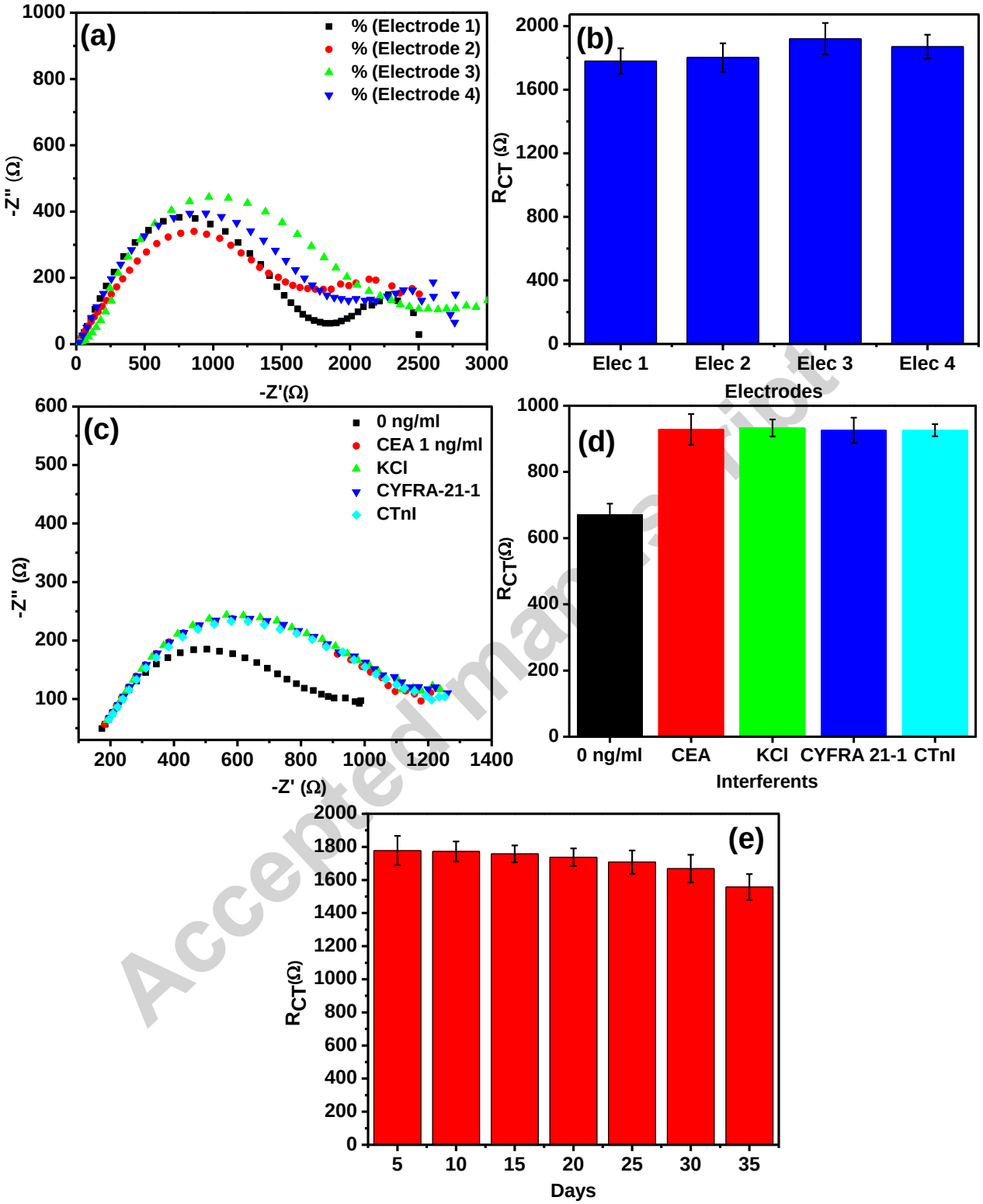

Fig.7. (a), (b) EIS responses of four independently fabricated BSA/anti-CEA/PBSE/Graphene/Cu electrodes in presence of 25.0 ng mL^{-1} CEA and their R_{CT} values, respectively, (c) and (d)

ACCEPTED MANUSCRIPT

Selectivity study of BSA/anti-CEA/PBSE/Graphene/Cu electrode in presence of different interferents such as: KCl, CYFRA-21-1 and CTnI (e) Storage stability of BSA/anti-CEA/PBSE/Graphene/Cu electrodes at regular interval of 5 days till 35 days.

The storage stability of the BSA/anti-CEA/PBSE/Graphene/Cu immunoelectrode has also been monitored by measuring EIS response in presence of 25.0 ng mL^{-1} CEA with a regular interval of 5 days (Fig. 7(e)). The immunoelectrode retains its activity upto 30 days with the decrement in R_{CT} of 6.13% when stored in refrigerated conditions at 4 ºC. After 35 days, 12.37 % decrement in R_{CT} values was found, this indicates that the storage stability of the fabricated immunoelectrodes is 30 days.

Table1. Comparison of sensing behavior of proposed bioelectrode with the other reported works.

S.No.	Substrate	Materials	Fabrication Method	Detection Method	Linear Range	Detection Limit	Reference
1	GCE	MWCNT, Chitosan, Glutaraldehyde, THAMP, Ferrocenecarboxylic acid, Dopamine, AuNPs, HRP	Drop cost	CV, EIS	0.01 – 80 ng mL^{-1}	0.002 ng mL^{-1}	(Feng et al. 2015)
2	Si/SiO_2	HRP, AuNPs, Carboxylic magnetic beads, Graphene, Hexacyanoferrate	Drop cost	EIS	5-60 ng mL^{-1}	5.0 ng mL^{-1}	(Jin et al. 2014)
3	GCE	AuNPs, MWCNTs, Chitosan	Drop cost	CV, EIS, DPV	0.3-2.5 ng mL^{-1} and 2.5-20 ng mL^{-1}	0.01 ng mL^{-1}	(Huang et al. 2010)
4	GCE	AuNPs,	Dip coating	CV, EIS,	1 fg mL^{-1} – 10	0.015 fg	(Liu and

ACCEPTED MANUSCRIPT

		PATP, hexacyanoferrates		DPV	ng mL^{-1}	mL^{-1}	Ma 2013)
5	Cu film	Graphene	Dip Coating	EIS	1.0 – 25.0 ng mL^{-1}	0.23 ng mL^{-1}	Present Work

The comparison of present work with the other reports (shown in Table-1) suggests that our biosensor is highly sensitive, selective and linear in the physiological range.

4. Conclusions

In the present study, we have fabricated anti-CEA/PBSE/Graphene/Cu immunosensing platform for sensitive and specific detection of cancer related biomarker CEA using EIS technique. Graphene has been synthesized on Cu film using CVD technique and anti-CEA has been immobilized over it using PBSE as a linker. The EIS studies of the fabricated electrodes reveal the sensitivity of 563.4 Ω ng^{-1} mL cm^{-2} with detection limit of 0.23 ng mL^{-1}, which meets the requirements of clinical diagnosis of cancer. Due to high sensitivity, specificity, ease of fabrication, and short analysis time this biosensor could be applied as potential candidate for clinical diagnosis of cancer at its early stage. It would be interesting to utilize this bioelectrode equipped with specific recognition elements for detection of other biomolecules too.

Acknowledgements

V.K.S. acknowledges UGC for providing Junior Research Fellowship (Fellowship Grant No: F.25-1/2014-15/(BSR)/5-127/2007/(BSR)). S.S. acknowledges DST, for the financial support (DST/INSPIRE Faculty Award/2014/MS-34). A.S. acknowledges DST, India for funding (Project Code: DST/TSG/PT/2012/68), DST-SERB India (Project Code: EMR/2016/007720), DST-PURSE-5050 and BHU.

Accepted manuscript

ACCEPTED MANUSCRIPT

References:

Ajayan, P.M., Tour, J.M., 2007. Materials science: nanotube composites. Nature 447(7148), 1066-1068.

Allen, B.L., Kichambare, P.D., Star, A., 2007. Carbon nanotube field-effect-transistor-based biosensors. Advanced Materials 19(11), 1439-1451.

Aquino, A., Formica, V., Prete, S.P., Correale, P.P., Massara, M.C., Turriziani, M., De Vecchis, L., Bonmassar, E., 2004. Drug-induced increase of carcinoembryonic antigen expression in cancer cells. Pharmacological research 49(5), 383-396.

Chae, S.J., Güneş, F., Kim, K.K., Kim, E.S., Han, G.H., Kim, S.M., Shin, H.J., Yoon, S.M., Choi, J.Y., Park, M.H., 2009. Synthesis of large-area graphene layers on poly-nickel substrate by chemical vapor deposition: wrinkle formation. Advanced Materials 21(22), 2328-2333.

Chen, R.J., Zhang, Y., Wang, D., Dai, H., 2001. Noncovalent sidewall functionalization of single-walled carbon nanotubes for protein immobilization. Journal of the American Chemical Society 123(16), 3838-3839.

Duffy, M.J., 2001. Carcinoembryonic antigen as a marker for colorectal cancer: is it clinically useful? Clinical chemistry 47(4), 624-630.

Feng, L., Chen, Y., Ren, J., Qu, X., 2011. A graphene functionalized electrochemical aptasensor for selective label-free detection of cancer cells. Biomaterials 32(11), 2930-2937.

Feng, L., Wu, L., Qu, X., 2013. New horizons for diagnostics and therapeutic applications of graphene and graphene oxide. Advanced Materials 25(2), 168-186.

Feng, T., Qiao, X., Wang, H., Sun, Z., Hong, C., 2015. Multi-walled carbon nanotubes–chitosan with a branched structure modified with ferrocenecarboxylic acid for carcinoembryonic antigen detection. Analytical Methods 7(23), 10032-10039.

Ferrari, A., Meyer, J., Scardaci, V., Casiraghi, C., Lazzeri, M., Mauri, F., Piscanec, S., Jiang, D., Novoselov, K., Roth, S., 2006. Raman spectrum of graphene and graphene layers. Physical review letters 97(18), 187401.

Ge, S., Ge, L., Yan, M., Song, X., Yu, J., Huang, J., 2012. A disposable paper-based electrochemical sensor with an addressable electrode array for cancer screening. Chemical Communications 48(75), 9397-9399.

Geim, A.K., 2009. Graphene: status and prospects. science 324(5934), 1530-1534.

Hansen, J.A., Wang, J., Kawde, A.-N., Xiang, Y., Gothelf, K.V., Collins, G., 2006. Quantum-dot/aptamer-based ultrasensitive multi-analyte electrochemical biosensor. Journal of the American Chemical Society 128(7), 2228-2229.

Huang, K.-J., Niu, D.-J., Xie, W.-Z., Wang, W., 2010. A disposable electrochemical immunosensor for carcinoembryonic antigen based on nano-Au/multi-walled carbon nanotubes–chitosans nanocomposite film modified glassy carbon electrode. Analytica chimica acta 659(1), 102-108.

Huang, Y., Dong, X., Liu, Y., Li, L.-J., Chen, P., 2011. Graphene-based biosensors for detection of bacteria and their metabolic activities. Journal of Materials Chemistry 21(33), 12358-12362.

Accepted manuscript

ACCEPTED MANUSCRIPT

Jin, B., Wang, P., Mao, H., Hu, B., Zhang, H., Cheng, Z., Wu, Z., Bian, X., Jia, C., Jing, F., 2014. Multi-nanomaterial electrochemical biosensor based on label-free graphene for detecting cancer biomarkers. Biosensors and Bioelectronics 55, 464-469.

Jung, J.H., Cheon, D.S., Liu, F., Lee, K.B., Seo, T.S., 2010. A graphene oxide based immuno-biosensor for pathogen detection. Angewandte Chemie International Edition 49(33), 5708-5711.

Kumar, S., Jagadeesan, K.K., Joshi, A.G., Sumana, G., 2013. Immuno-CoPS (conducting paper strips) for futuristic cost-effective cancer diagnostics. Rsc Advances 3(29), 11846-11853.

Kumar, S., Kumar, S., Srivastava, S., Yadav, B.K., Lee, S.H., Sharma, J.G., Doval, D.C., Malhotra, B.D., 2015. Reduced graphene oxide modified smart conducting paper for cancer biosensor. Biosensors and Bioelectronics 73, 114-122.

Lee, C., Wei, X., Kysar, J.W., Hone, J., 2008. Measurement of the elastic properties and intrinsic strength of monolayer graphene. science 321(5887), 385-388.

Liu, Y., Dong, X., Chen, P., 2012. Biological and chemical sensors based on graphene materials. Chemical Society Reviews 41(6), 2283-2307.

Liu, Y., Yuan, L., Yang, M., Zheng, Y., Li, L., Gao, L., Nerngchamnong, N., Nai, C.T., Sangeeth, C.S., Feng, Y.P., 2014. Giant enhancement in vertical conductivity of stacked CVD graphene sheets by self-assembled molecular layers. Nature communications 5, 5461.

Liu, Z., Ma, Z., 2013. Fabrication of an ultrasensitive electrochemical immunosensor for CEA based on conducting long-chain polythiols. Biosensors and Bioelectronics 46, 1-7.

Loewenstein, M., Zamcheck, N., 1978. Carcinoembryonic antigen (CEA) levels in benign gastrointestinal disease states. Cancer 42(S3), 1412-1418.

Malard, L., Pimenta, M., Dresselhaus, G., Dresselhaus, M., 2009. Raman spectroscopy in graphene. Physics Reports 473(5), 51-87.

Mishra, M., Gundimeda, A., Krishna, S., Aggarwal, N., Gahtori, B., Dilawar, N., Aggarwal, V.V., Singh, M., Rakshit, R., Gupta, G., 2017. Wet chemical etching induced stress relaxed nanostructures on polar & non-polar epitaxial GaN films. Physical Chemistry Chemical Physics 19(13), 8787-8801.

Moisel, M., de Mele, M.L., Müller, W.D., 2008. Biomaterial interface investigated by electrochemical impedance spectroscopy. Advanced engineering materials 10(10), B33-B46.

Neto, A.C., Guinea, F., Peres, N., Novoselov, K.S., Geim, A.K., 2009a. The electronic properties of graphene. Reviews of modern physics 81(1), 109.

Novoselov, K.S., Geim, A.K., Morozov, S.V., Jiang, D., Zhang, Y., Dubonos, S.V., Grigorieva, I.V., Firsov, A.A., 2004. Electric field effect in atomically thin carbon films. science 306(5696), 666-669.

Randles, J.E.B., 1947. Kinetics of rapid electrode reactions. Discussions of the faraday society 1, 11-19.

Schniepp, H.C., Li, J.-L., McAllister, M.J., Sai, H., Herrera-Alonso, M., Adamson, D.H., Prud'homme, R.K., Car, R., Saville, D.A., Aksay, I.A., 2006. Functionalized single graphene sheets derived from splitting graphite oxide. The Journal of Physical Chemistry B 110(17), 8535-8539.

Accepted manuscript

ACCEPTED MANUSCRIPT

Setti, L., Fraleoni-Morgera, A., Ballarin, B., Filippini, A., Frascaro, D., Piana, C., 2005. An amperometric glucose biosensor prototype fabricated by thermal inkjet printing. Biosensors and Bioelectronics 20(10), 2019-2026.

Singh, C., Srivastava, S., Ali, M.A., Gupta, T.K., Sumana, G., Srivastava, A., Mathur, R., Malhotra, B.D., 2013. Carboxylated multiwalled carbon nanotubes based biosensor for aflatoxin detection. Sensors and Actuators B: Chemical 185, 258-264.

Singh, R., Hong, S., Jang, J., 2017. Label-free detection of influenza viruses using a reduced graphene oxide-based electrochemical immunosensor integrated with a microfluidic platform. Scientific reports 7, 42771.

Srivastava, A., Galande, C., Ci, L., Song, L., Rai, C., Jariwala, D., Kelly, K.F., Ajayan, P.M., 2010. Novel liquid precursor-based facile synthesis of large-area continuous, single, and few-layer graphene films. Chemistry of Materials 22(11), 3457-3461.

Su, F., Xu, C., Taya, M., Murayama, K., Shinohara, Y., Nishimura, S.-I., 2008. Detection of carcinoembryonic antigens using a surface plasmon resonance biosensor. Sensors 8(7), 4282-4295.

Sui, Y., Appenzeller, J., 2009. Screening and interlayer coupling in multilayer graphene field-effect transistors. Nano letters 9(8), 2973-2977.

Wanekaya, A.K., Chen, W., Myung, N.V., Mulchandani, A., 2006. Nanowire-based electrochemical biosensors. Electroanalysis 18(6), 533-550.

Yang, C., Xu, C., Wang, X., Hu, X., 2012. Quantum-dot-based biosensor for simultaneous detection of biomarker and therapeutic drug: first steps toward an assay for quantitative pharmacology. Analyst 137(5), 1205-1209.

Yang, J., Pang, F., Zhang, R., Xu, Y., He, P., Fang, Y., 2008. Electrochemistry and Electrocatalysis of Hemoglobin on 1-Pyrenebutanoic Acid Succinimidyl Ester/Multiwalled Carbon Nanotube and Au Nanoparticle Modified Electrode. Electroanalysis 20(19), 2134-2140.

Yang, M., Gong, S., 2010. Immunosensor for the detection of cancer biomarker based on percolated graphene thin film. Chem. Commun. 46(31), 5796-5798.

Yang, W., Ratinac, K.R., Ringer, S.P., Thordarson, P., Gooding, J.J., Braet, F., 2010. Carbon nanomaterials in biosensors: should you use nanotubes or graphene? Angewandte Chemie International Edition 49(12), 2114-2138.

Yeh, C.-H., Kumar, V., Moyano, D.R., Wen, S.-H., Parashar, V., Hsiao, S.-H., Srivastava, A., Saxena, P.S., Huang, K.-P., Chang, C.-C., 2016. High-performance and high-sensitivity applications of graphene transistors with self-assembled monolayers. Biosensors and Bioelectronics 77, 1008-1015.

Zhang, B., Cui, T., 2011. An ultrasensitive and low-cost graphene sensor based on layer-by-layer nano self-assembly. Applied Physics Letters 98(7), 073116.

Zhang, G.-J., Huang, M.J., Liu, E.T., Desai, K.V., 2011. Self-assembled monolayer-assisted silicon nanowire biosensor for detection of protein–DNA interactions in nuclear extracts from breast cancer cell. Biosensors and Bioelectronics 26(7), 3233-3239.

Accepted manuscript

ACCEPTED MANUSCRIPT

Zhang, G.-J., Luo, Z.H.H., Huang, M.J., Tay, G.K.I., Lim, E.-J.A., 2010a. Morpholino-functionalized silicon nanowire biosensor for sequence-specific label-free detection of DNA. Biosensors and Bioelectronics 25(11), 2447-2453.

Zhang, G.-J., Zhang, L., Huang, M.J., Luo, Z.H.H., Tay, G.K.I., Lim, E.-J.A., Kang, T.G., Chen, Y., 2010b. Silicon nanowire biosensor for highly sensitive and rapid detection of Dengue virus. Sensors and Actuators B: Chemical 146(1), 138-144.

Zhang, S., Wright, G., Yang, Y., 2000. Materials and techniques for electrochemical biosensor design and construction. Biosensors and Bioelectronics 15(5), 273-282.

Zheng, G., Lieber, C.M., 2011. Nanowire biosensors for label-free, real-time, ultrasensitive protein detection. Nanoproteomics, pp. 223-237. Springer.

Zheng, G., Patolsky, F., Cui, Y., Wang, W.U., Lieber, C.M., 2005. Multiplexed electrical detection of cancer markers with nanowire sensor arrays. Nature biotechnology 23(10), 1294-1301.

Zhou, M., Zhai, Y., Dong, S., 2009. Electrochemical sensing and biosensing platform based on chemically reduced graphene oxide. Analytical chemistry 81(14), 5603-5613.

Graphical Abstracts